Dosimetric and kinetic investigations of γ-irradiated sodium tartrate dihydrate

H. Tuner & M. A. Kayıkçı

Radiation and Environmental Biophysics

ISSN 0301-634X
Volume 51
Number 1

Radiat Environ Biophys (2012) 51:61-67
DOI 10.1007/s00411-011-0392-7

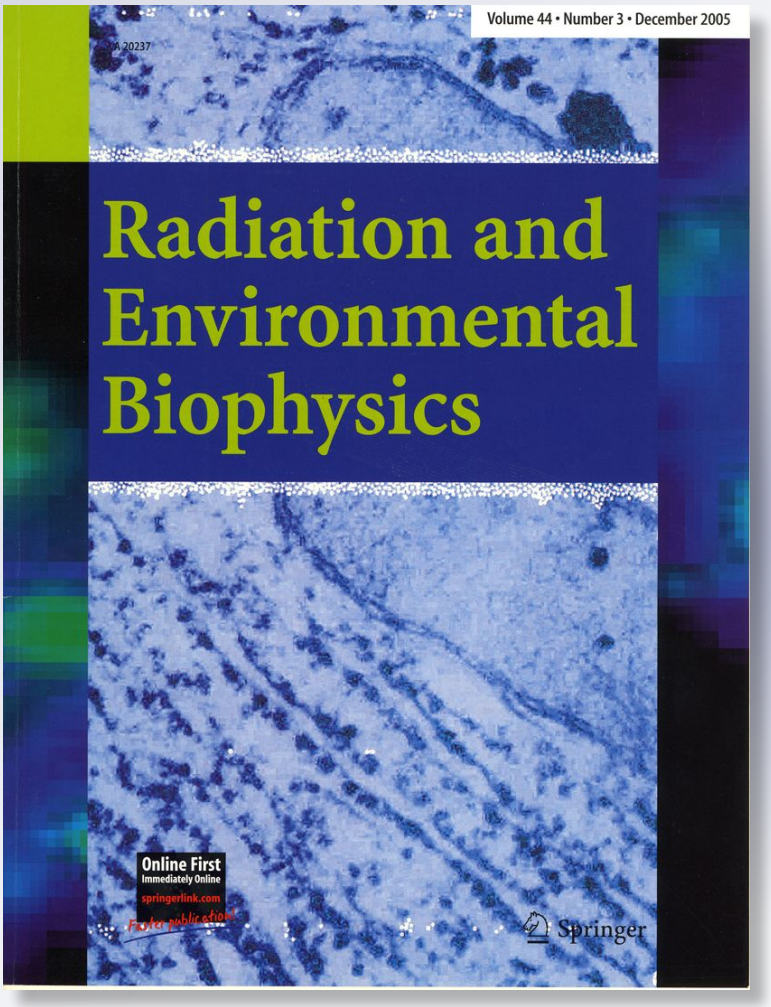

Springer

Your article is protected by copyright and all rights are held exclusively by Springer-Verlag. This e-offprint is for personal use only and shall not be self-archived in electronic repositories. If you wish to self-archive your work, please use the accepted author's version for posting to your own website or your institution's repository. You may further deposit the accepted author's version on a funder's repository at a funder's request, provided it is not made publicly available until 12 months after publication.

Springer

Author's personal copy

Radiat Environ Biophys (2012) 51:61–67
DOI 10.1007/s00411-011-0392-7

ORIGINAL PAPER

Dosimetric and kinetic investigations of γ-irradiated sodium tartrate dihydrate

H. Tuner · M. A. Kayıkçı

Received: 23 May 2011 / Accepted: 15 October 2011 / Published online: 4 November 2011
© Springer-Verlag 2011

Abstract Effects of gamma radiation on solid sodium tartrate dihydrate (NaTA) were studied using electron spin resonance (ESR) spectroscopy. One main singlet located at $g = 2.0034$ and many weak lines located at low and high magnetic field sides were found in the irradiated samples. Dosimetric and kinetic features of the radical species responsible for the experimental ESR spectra were explored through the variations in the signal intensities with respect to applied microwave power, temperature and storage time. Activation energies of the involved radical species were also determined using data derived from annealing studies.

Introduction

Electron spin resonance (ESR) spectroscopy has been successfully used in the detection of radiation-induced species that have unpaired electrons, and in the determination of the kinetic behavior of these species. ESR has been applied at medium- and high-dose ranges using L-alanine as a dosimeter (Bradshaw et al. 1962; Regulla and Deffner 1982; Kojima and Tanaka 1989; Ikeya 1993). Although studies carried out by different research groups on alanine were promising in measuring low radiation doses (Anton 2006; Castro et al. 2006; Sharpe 2003, Sharpe et al. 1996), it would be interesting to explore new materials if ESR is to become a serious alternative to existing methods of dose measurement. In this respect, such materials should show a high radical yield, a linear dose–response curve, sharp spectral lines, radicals that are stable at room temperature (Ikeya et al. 2000; Lund et al. 2002) and that show simple ESR spectra. In this regard, sugar, ammonium tartrate, 2-methylalanine, compounds of formic acid and dithionate salts have been evaluated in the literature (Ikeya et al. 2000; Hassan and Ikeya 2000; Olsson et al. 2000; Murali et al. 2001; Yordanov et al. 2002; Lund et al. 2002; Vestad et al. 2003; Gustafsson et al. 2004; Yordanov and Gancheva 2004; Gancheva et al. 2006; Karakirova et al. 2010).

Spectroscopic features of the radical species produced in dl-tartaric acid (dl-TA) single crystals, which were irradiated with gamma and X-rays at room temperature, 77 and 195 K, have been reported in the literature (Narasimha Rao and Gordy 1962; Moulton and Cernansky 1969, 1970). Three different radicals that have different spectroscopic features and which are produced upon irradiation of the dl-TA single crystal have been proposed (Narasimha Rao and Gordy 1962; Moulton and Cernansky 1969, 1970). Kinetic and dosimetric features of polycrystalline dl-TA at low (50–1,000 Gy) and medium (1–25 kGy) dose ranges were determined in two studies (Tuner and Korkmaz 2009; Korkmaz et al. 2010). The radical species produced upon the irradiation of dl-TA and its ammonium salt were proposed to be radical I giving rise to a doublet with relatively high hyperfine splitting, radical II that produces a slightly anisotropic doublet with small hyperfine splitting (0.65 mT) and radical III that presents a spectrum with four resonance lines.

In the present work, the kinetic features of the radicalic intermediates produced upon gamma-irradiated sodium salt of dl-tartaric acid (NaTA) were investigated through a detailed ESR study performed at room and high temperatures. The dosimetric potential of NaTA in a medium (0.5–20 kGy) dose range is also investigated.

H. Tuner (✉) · M. A. Kayıkçı
Department of Physics, Faculty of Art and Science, Balikesir University, 10145 Cagis, Balikesir, Turkey
e-mail: htuner@hacettepe.edu.tr

Author's personal copy

Materials and methods

Sodium tartrate dihydrate (NaTA) or chemically 2.3-dihydroxy sodium succinate is a water-soluble sodium salt of tartaric acid. NaTA is a colorless crystal or a white crystalline powder with a melting point of about 420 K. NaTA crystallizes as orthorhombic with a space group $P2_12_12_1$, and there are four molecules in the unit cell (Ramachandran and Radhakrishnan 1951; Ambady and Kartha 1968). It is used as an emulsifier (E335) and a binding agent in food products such as jellies, margarine and sausage casings (Lide 1998; JECFA 1978, 2000; Vickers et al. 2007; FASEB 1979; EFSA 2003). It is also a common standard to assay water content for Karl Fischer titration (Neuss et al. 1951; William and Bhaskara 1976). In the present work, NaTA crystalline powder was provided from Aldrich and used without any further treatment by keeping it in sealed polyethylene vials at room temperature (290 K) before irradiation. The molecular structure of NaTA is given in Fig. 1. All irradiations were performed at room temperature (290 K) using a ^{60}Co-γ source supplying a dose rate of 0.8 kGy/h. The dose rate at the sample site was measured by a Fricke ferrous sulfate dosimeter. A set of samples irradiated at doses of 0.5, 1.0, 2.0, 5.0, 7.0, 10.0, 15.0 and 20.0 kGy were employed to construct a dose–response curve. Samples irradiated at a dose of 10 kGy were used to investigate the kinetic features of the contributing radical species.

ESR measurements were carried out on samples transferred to quartz ESR tubes of 4 mm inner diameter using a Bruker EMX-131 X-band ESR spectrometer operating at 9.8 GHz and equipped with a high-sensitive cylindrical cavity and an NMR teslameter that allowed the measurement of the actual magnetic field at the site of the sample. Thus, the g value could be determined directly from the recorded spectra. A crystalline DPPH (1,1-diphenyl-2-picryl-hydrazyl) sample was used as a standard sample ($g = 2.0036$) to confirm the g value of the studied sample. The operation conditions (Table 1) for room and low temperatures were determined from microwave power studies derived at room (290 K) and low (130 K) temperatures. Signal intensities were measured directly from the recorded first derivative spectra, and the spectrum area below the absorption curves, which is proportional to the number of the radicals present in the sample, was calculated by the double integration technique using the Bruker WINEPR program (Barr et al. 1998). Sample temperature inside the microwave cavity was monitored with a digital temperature control unit (Bruker ER 411-VT) which provided the opportunity of measuring the temperature with an accuracy of ± 0.5 K at the site of the sample. Cooling, heating and subsequent cooling cycles were adopted to monitor free radical signals over a large temperature range. The temperature of the samples was first decreased to 130 K, starting from room temperature with an increment of 20 K, then was increased to 370 K, and finally was decreased again to room temperature.

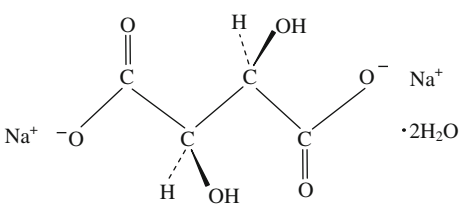

Fig. 1 Molecular structure of sodium tartrate dihydrate

Table 1 Spectrometer operation conditions adopted during the experiments

	Room temperature	Low temperature
Central field (mT)	351.4	335.9
Scan range (mT)	7	7
Microwave power (mW)	0.4	0.01
Microwave frequency (GHz)	9.86	9.42
Receiver gain ($\times 10^4$)	1.0	1.0
Modulation frequency (kHz)	100	100
Modulation amplitude (mT)	0.1	0.1
Time constant (ms)	327.68	327.68
Sweep time (s)	83.89	83.89

The kinetic behavior of the involved radical species was evaluated at four different temperatures (320, 325, 330 and 335 K). To achieve this, the samples were heated to a predetermined temperature and kept at this temperature for about 5 min to reach thermal equilibrium; then, spectra were recorded at intervals of 2 min without cooling the samples to room temperature. All results are given as the mean of three different measurements performed using three different samples.

Results and discussion

While unirradiated NaTA showed no ESR signal, irradiated polycrystalline of NaTA was observed to show an ESR spectrum consisting of one main strong resonance line with many weak lines (Fig. 2) spread over a magnetic field range of 7 mT and centered at about $g = 2.0034$. The main strong resonance line (I_2) seems to be a singlet or unresolved doublet with narrow line width ($\sim$0.6 mT), and it is dominating the ESR spectrum of irradiated NaTA. The weak line I_1, which is located at both sides of the strong line, has a doublet with high hyperfine splitting ($\sim$2.4 mT). The ESR spectrum of irradiated NaTA also has very weak lines (I_3) that are located at both the low and

Author's personal copy

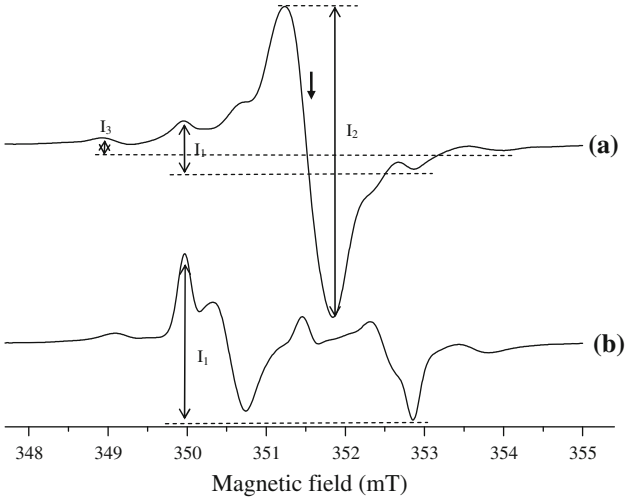

Fig. 2 ESR spectra of NaTA. **a** Irradiated at 10 kGy, **b** annealed at 335 K for 1 h. *Arrow* indicates the position of the DPPH resonance line ($g = 2.0036$)

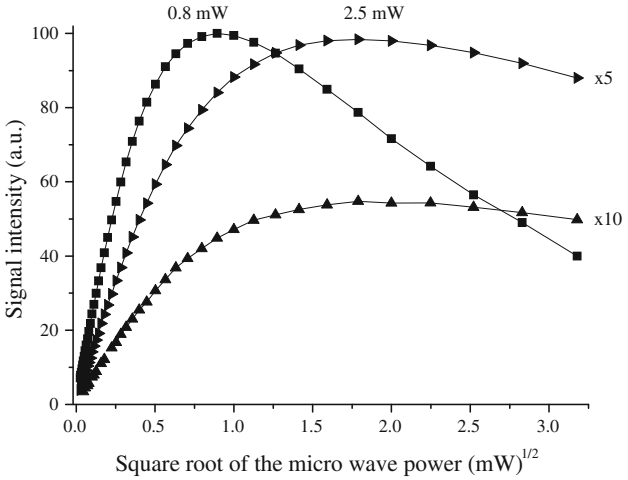

Fig. 3 Microwave saturation at room temperature for I_1 (*filled triangle right*), I_2 (*filled square*) and I_3 (*filled triangle*) intensities, for a sample irradiated at a dose of 10 kGy

high magnetic field side. These preliminary findings show that the radicals produced in irradiated NaTA were the same as the radicals produced in dl-TA and ammonium tartrate. The weak line that is denoted as I_3 seems to form the two lines of the quartet signal (Fig. 2b). The other two lines of the same quartet signal were screened by the strong resonance line.

Variations in the signal intensities with microwave power

Samples irradiated at a dose of 10 kGy were used to determine the microwave power saturation features of associated radical species. Variations in the assigned line intensities with microwave power were investigated both at 290 K and at 130 K in the ranges of 6.4×10^{-4}–10.0 and 2.0×10^{-4}–0.4 mW, respectively. The strong resonance line (I_2) exhibited the characteristic behavior of a homogeneously broadened resonance line both at room temperature and at 130 K. It started to increase at low microwave powers, and I_2 reached its maximum value at about 0.80 mW, and then started to decrease at high powers (Fig. 3). The other two lines, which are denoted as I_1 and I_3, showed almost the same variation with microwave power: At room temperature, I_1 and I_3 reached their maximum value at 2.5 mW, and they exhibited the characteristic behavior of an inhomogeneously broadened resonance line (Fig. 3). At 130 K, they showed the same saturation behavior but at lower microwave power values.

The behavior of the irradiated samples on variation in the amplitude modulation showed that there was no significant change on the experimental spectra, except an increase in the signal intensity in the range of 0.01–0.15 mT.

Table 2 Mathematical functions, parameter values and correlation coefficients (r^2) best describing the experimental dose–response data

Functions	Spectrum area	I_1	I_2
$I = a + b \cdot D$			
a	50.940	1.041	12.479
b	76.760	1.390	7.856
r^2	0.99285	0.98775	0.97686
$I = c + f \cdot D + g \cdot D^2$			
c	0	−0.159	0
f	99.685	1.920	12.927
g	−1.170	−0.027	−0.253
r^2	0.99904	0.99738	0.99920
$I = h \cdot D^k$			
h	116.841	2.230	17.970
k	0.863	0.846	0.736
r^2	0.99703	0.99348	0.99478
$I = m \cdot (1 - e^{-n \cdot D})$			
m	3,434.366	55.406	221.642
n	0.029	0.035	0.063
r^2	0.99885	0.99669	0.99944

Dose–response curves

ESR spectroscopy is commonly used for dose measurement and may provide important information about the discrimination of irradiated and unirradiated samples. For this purpose, the mathematical functions that best describe the dose–response curves should be determined, and linear, polynomial and exponential functions are frequently used (Dodd et al. 1988; Desrosiers 1991, Desrosiers et al. 1991; Basly et al. 1998; Polat and Korkmaz 2005; Tuner and Korkmaz 2009; Ustundag and Korkmaz 2009). Samples

Author's personal copy

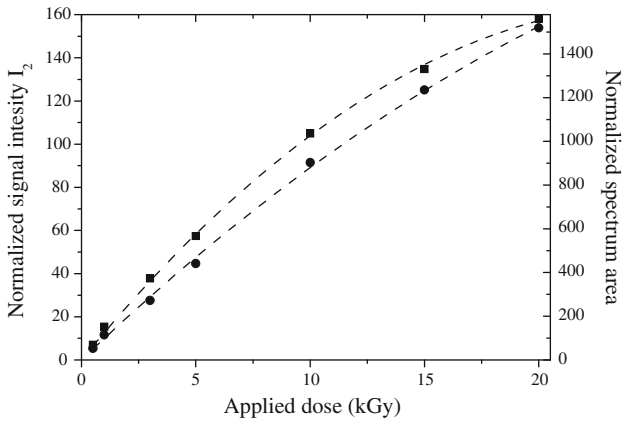

Fig. 4 Variation in the dominant normalized signal intensity I_2 (*filled square*, *left y-axis*) and spectrum area (*filled circle*, *right y-axis*) with applied radiation dose. *Dashed lines* calculated using polynomial function (see Table 2)

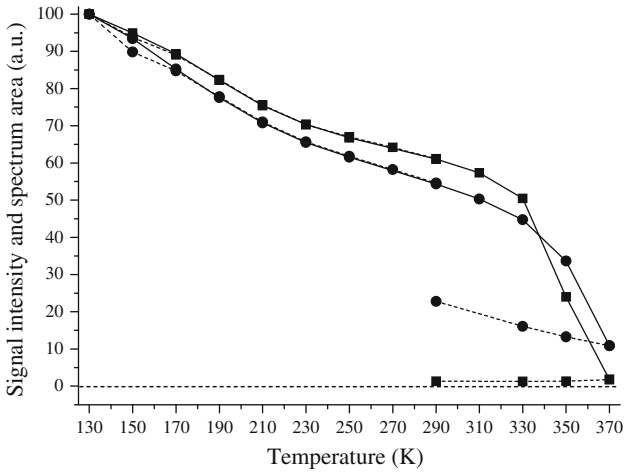

Fig. 5 Variation in the spectrum area (*filled circle*) and I_2 intensity (*filled square*) with temperature for a sample irradiated at 10 kGy. (Cooling: from 290 to130 K and from 370 to 290 K (*dashed lines*); heating from 130 to 370 K (*solid lines*))

irradiated at doses of 0.5, 1.0, 2.0, 5.0, 7.0, 10.0, 15.0, and 20.0 kGy were used here to construct dose–response curves. Measured signal intensities and spectrum areas calculated from recorded spectra were normalized to mass of samples and spectrometer gain. Mathematical functions that are given in Table 2 were tried to fit the experimental dose–response data obtained in the present work. The results are presented in Fig. 4. It is concluded that a linear-quadratic function of the applied dose, that is, a function of the type $I = c + f \cdot D + g \cdot D^2$ where I and D are the intensity and applied dose in kGy, respectively, and c, f and g are fitted parameters, describes the experimental data best.

Signal intensities of the other measured lines (I_1 and I_3) are very low compared with the signal intensity of I_2. Therefore, only the results for I_2 and spectrum area are given in Fig. 4.

Variable-temperature effects on signal intensities and radicals

Variations in the monitored I_2 intensity (Fig. 2b) and spectrum area with temperature were investigated in the temperature range of 130–370 K using a sample irradiated with a dose of 10 kGy. To avoid saturation effects, even at the lowest temperature achievable in the present work (130 K), care was taken with the use of microwave power. Thus, the spectrometer operation conditions given in Table 1 for the low temperature were adopted throughout the variable-temperature studies. Cooling the sample to 130 K produced an intensity increase that was similar for all lines. The variation in spectrum area, which is proportional to the total number of the produced radicals, and dominant line intensity I_2 are illustrated in Fig. 5. The signal intensities and the spectrum area were normalized to their values at 130 K for comparison. Heating the sample again to room temperature showed reversible changes, and the measured intensities and spectrum area reached their initial values before cooling. In contrast, heating the sample above room temperature produced irreversible decreases in the signal intensity (I_2) and spectrum area (Fig. 5). Note that the decrease in the signal intensity and in spectrum area was found to be different. While the signal I_2 decayed and its intensity decreased dramatically at about 330 K, the signal intensity of I_1 started to increase at the same temperature. This behavior is an indication of the transformation of the radical II (that is responsible for I_2) to the radical I (responsible for I_1). While I_2 almost completely disappeared at 370 K, the signal I_1 was still distinguishable from background. Cooling the sample to 290 K did not affect the signal intensity of I_2, but the spectrum area values increased (Fig. 5). From these irreversible changes, it is concluded that the total number of radicals decreased above room temperature.

Kinetic behavior of the produced radicals

Irreversible decreases and dramatic changes in ESR intensities of the spectra at high temperatures prompted us to investigate the behavior of the radical species contributing to the formation of the experimental spectrum after irradiation of NaTA. Variations in the line intensities and spectrum area at high temperatures were studied, to obtain information about the kinetic features of the radicals produced in irradiated NaTA. Data derived from a sample irradiated at 10 kGy, which are annealed, which were at four different temperatures (320, 325, 330 and 335 K), are given in Fig. 6a and b for the I_1 and I_2 resonance lines,

Author's personal copy

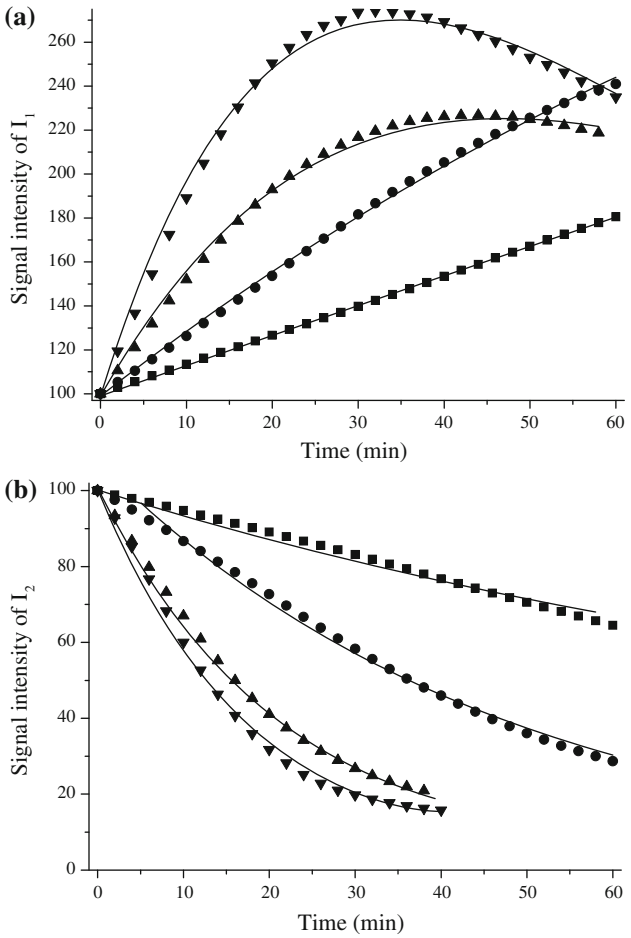

Fig. 6 Variation in the measured signal intensities for a sample irradiated at a dose of 10 kGy with annealing time at four different temperatures. **a** I_1 and **b** I_2. *Symbols* represent experimental data (*filled square* (320 K), *filled circle* (325 K), *filled triangle* (330 K), *filled triangle down* (335 K)); *solid lines* represent theoretical data (calculated using parameters given in Table 3)

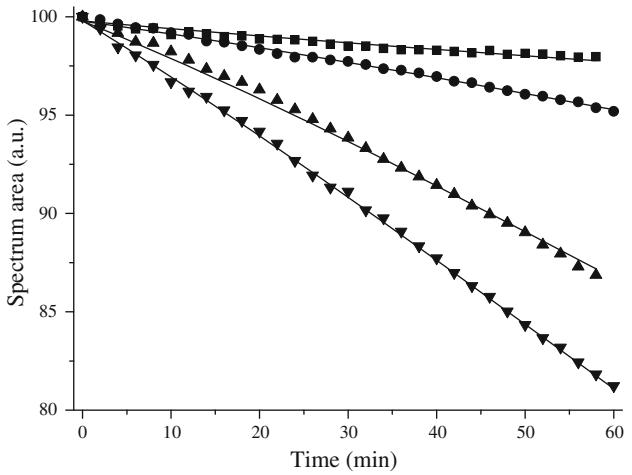

Fig. 7 Variation in the spectrum area for a sample irradiated at a dose of 10 kGy with annealing time at four different temperatures. *Symbols* represent experimental data (*filled square* (320 K), *filled circle* (325 K), *filled triangle* (330 K), *filled triangle down* (335 K)); *solid lines* represent theoretical data (calculated using parameters given in Table 3)

respectively, and in Fig. 7 for the spectrum area. While the signal intensity of I_2 rapidly decreased at all temperatures (Fig. 6b), the signal intensity of I_1 first increased and then decreased continuously (Fig. 6a). The increase in I_1 shows that there is a transformation from one radical to another. Evaluation of the spectrum area at the four different temperatures showed that the radicals decay with relatively low decay rates (Fig. 7). Consequently, while the radical responsible for the signal I_2 decays, it also transforms to another radical that is responsible for the signal I_1. The spectrum area and increase in the intensity of I_1 showed that the transformation rate is faster than its decay. Similarly, below 330 K, and at the beginning of the annealing studies ($\sim$25 min) above 330 K, the formation of the radical responsible for I_1 was faster than its decay.

This transformation-generation behavior seems to be the similar mechanism that was reported in the literature for dl-TA irradiated at a low temperature and heated to room temperature (Narasimha Rao and Gordy 1962; Moulton and Cernansky 1969, 1970), and for dl-TA irradiated at low radiation doses (Tuner and Korkmaz 2009). For example, after irradiation of dl-TA, the radical III which includes a quartet of ESR lines transforms to the radical II which is a doublet with small hyperfine splitting (Narasimha Rao and Gordy 1962; Moulton and Cernansky 1969, 1970). This transformation is relatively fast for irradiated dl-TA. In contrast, it is shown here that for irradiated NaTA, the radical responsible for signal I_2 (radical II) transforms to the radical responsible for signal I_1 (radical I). It is concluded that this different transformation-formation mechanism is probably due to the different crystal matrix and different electronic configurations of NaTA.

In the present study, the radical II transforms to the radical I. The radical II is observed to decay with two different modes. The rate of the first decay mode, which is the mode that ends with an ESR-silent species, is determined by the partial decay constant k_a, while the rate of decay into another mode, which ends with radical I, is determined by the partial decay constant k_b. The decay rate for radical II is the sum of these two decay constants, $k_2 = k_a + k_b$, and the variation in the signal intensity I_2 (radical II) is as $I_{\mathrm{II}} = I_{20} \cdot \exp(-k_2 \cdot t)$ where I_{20} indicates the initial signal intensity/spectrum area. The increase–decrease mechanism of I_1 is supposed to be written as, $I_{\mathrm{I}} = I_{10} \cdot \exp(-k_1 \cdot t) + I_{21} \cdot \left(\frac{k_{21}}{k_1 - k_{21}}\right) \cdot [\exp(-k_1 \cdot t) - \exp(-k_{21} \cdot t)]$, where k_1 and k_{21} are describing the decay rate and the formation rate of the radical I, respectively.

As it is seen from Fig. 6a and b, the increase rate of signal I_1 is higher than the decrease rate of signal I_2. This difference is related to the different line widths of each

Author's personal copy

Table 3 Decay constants and activation energies calculated for responsible radical species at four different annealing temperatures

Radical species	Decay constants (min^{-1}) × 10^{-3}				Activation energy (kJ/mol)
	320 K	325 K	330 K	335 K	
I	0.24	1.12	4.01	8.47	213.72 ± 30.53
II	12.46	13.59	15.46	16.70	17.96 ± 4.68
III	0.11	0.41	1.20	4.63	219.10 ± 21.42

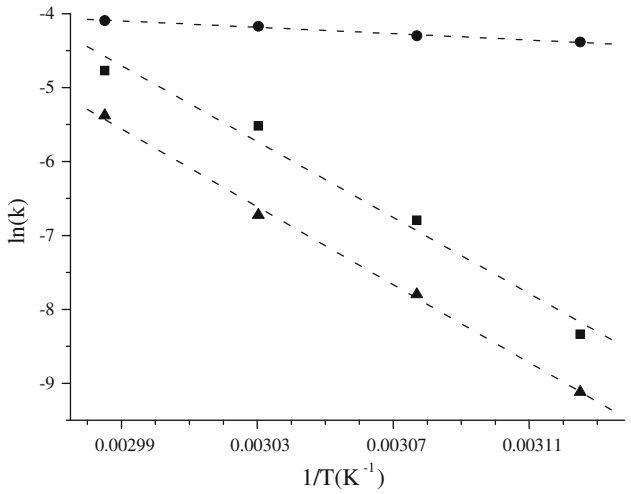

Fig. 8 Arrhenius plot of the decay constants derived from spectrum area calculations (*filled square* k1, *filled circle* k2, *filled triangle* k3)

signal. Thus, the line width of I_1 is smaller than that of I_2. A function that consists of the sum of I_I and I_{II} and another exponential decay function that describes the decay of radical III were used to describe the decay variations in the spectrum area (Table 3). The activation energies of each radical were calculated from the Arrhenius graph (Fig. 8) using the decay constants (k's) calculated for the involved radicals. The decay constants and activation energies of the involved species derived from the spectrum area are given in Table 3.

It is noted that when a sample irradiated at a dose of 10 kGy was stored at room temperature open to air over a storage period of 90 days, and its spectra were recorded in regular time intervals, similar variations in the signal intensities and transformation-generation behavior of the radicals were found, and only 25% of the total number of the radicals were decayed after 3 months of storage.

Conclusion

Gamma-irradiated NaTA exhibits an ESR spectrum with many resonance lines, where one main strong line dominates the spectrum. From the dosimetric material point of view, the narrow line width (~0.6 mT) of the main line, the acceptable saturation behavior with microwave power, and the almost linear dose–response at medium dose range (<10 kGy) seem to be the positive features of NaTA. On the other hand, however, the fast decay of signal intensity at high temperatures (>330 K) and the transformation of one type of radical to another even at room temperature are the negative features.

Although the kinetic behavior of NaTA is not favorable for a dosimetric material, it gives significant information about the decay-transformation behavior of the radiation-induced intermediates. A model based on decay and transformation-formation is adopted to determine this mechanism. The radical II almost completely decayed by two different modes after 40 min of annealing (Fig. 6b) above 330 K. This interpretation is supported by the finding of the variation in the signal I_2 (Fig. 6a). However, only 20% of the total number of radicals was decayed even after annealing at 335 K for 60 min (Fig. 7). The activation energy of radical II was found to be about 17.96, and 213.72 and 219.10 kJ/mol for radical I and radical III, respectively. As it is expected from its rapid decay, the activation energy of radical II is low. The same variations in the ESR spectra and signal intensities were observed after 3 months of storage time.

Despite the negative findings on the decay behavior of NaTA at room and high temperatures, ESR spectroscopy could be used for the discrimination of irradiated from unirradiated NaTA even after a storage period of 3 months.

Acknowledgments This work was supported by the Turkish Research Council (TUBITAK), grant no: 110T825.

References

Ambady GK, Kartha G (1968) The crystal and molecular structure of sodium D-tartrate. Acta Cryst B24:1540–1547

Anton M (2006) Uncertainties in alanine/ESR dosimetry at the Physikalisch-Technische Bundesanstalt. Phys Med Biol 51:5419–5440

Barr D, Jiang JJ, Weber R (1998) Performing double integrations using WIN-EPR. Bruker biospin report 6

Basly JP, Basly I, Bernard M (1998) Electron spin resonance identification of irradiated ascorbic acid: dosimetry and influence of powder fineness. Anal Chim Acta 372:373–378

Bradshaw WW, Cadena DG, Crawford GW, Spetzler HAW (1962) The use of alanine as a solid dosimeter. Radiat Res 17:11–21

Castro F, Ponte F, Pereira L (2006) Development of pysical and numerical techniques of alanine/EPR dosimetry in radiotherapy. Radiat Prot Dosim 122:509–512

Desrosiers MF (1991) Estimation of absorbed dose in radiation-processed food-2. Test of the EPR response function by an exponential fitting analysis. Appl Radiat Isot 42:617–619

Desrosiers MF, Wilson GL, Hunter CR, Hutton DR (1991) Estimation of the absorbed dose in radiation-processed food-1. Test of the EPR response function by a linear regression analysis. Appl Radiat Isot 42:613–616

Author's personal copy

Dodd NJF, Lea JS, Swallow AJ (1988) ESR detection of irradiated food. Nature 334:387–388

EFSA (2003) Opinion of the scientific panel on food additives, flavourings, processing aids and materials in contact with food (AFC) on a request from the commission related to L-carnitine-L-tartrate for use in foods for particular nutritional uses. EFSA J 19:1–13

FASEB (1979) Evaluation of the health aspects of potassium acid tartrate, sodium potassium tartrate, sodium tartrate and tartaric acid as food ingredients. Federation of American Societies for Experimental Biology (FASEB), Bethesda, MD, Life Sciences Research Ofice (LSRO). PB301403

Gancheva V, Sagstuen E, Yordanov ND (2006) Study on the EPR/dosimetric properties of some substituted alanines. Radiat Phys Chem 75:329–335

Gustafsson H, Olson S, Lund A, Lund E (2004) Ammonium formate, a compound for sensitive EPR dosimetry. Radiat Res 161:464–470

Hassan GM, Ikeya M (2000) Metal ion-organic compound for high sensitive ESR dosimetry. Appl Radiat Isot 52:1247–1254

Ikeya M (1993) New applications of electron spin resonance: dating, dosimetry, and microscopy. World Scientific Publishing Co., Singapore

Ikeya M, Hassan GM, Sasaoka H, Kinoshita Y, Takaki S, Yamanaka C (2000) Strategy for finding new materials for ESR dosimeters. Appl Radiat Isot 52:1209–1215

JECFA (1978) Tartaric acid and monosodium tartrate. Twenty-first report of the joint FAO/WHO expert committee on food additives. Technical report series 617:13–14. World Health Organization, Geneva

JECFA (2000) Safety evaluation of certain food additives and contaminants. 53rd Meeting of the Joint FAO/WHO Expert Committee on Food Additives (JECFA), June 1–10, 1999, Rome. World Health Organization (WHO), International Programme on Chemical Safety (IPCS); Geneva, Switzerland, WHO Food Additives series, no. 44

Karakirova Y, Yordanov ND, De Cooman H, Vrielinck H, Callens F (2010) Dosimetric characteristics of different types of saccharides: an EPR and UV spectrometric study. Radiat Phys Chem 79:654–659

Kojima T, Tanaka R (1989) Polymer-alanine dosimeter and compact reader. Int J Appl Radiat Isot 40:851–857

Korkmaz G, Polat M, Korkmaz M (2010) Usability of tartaric acid in dose measurements: an ESR study. Radiat Eff Defect S 165:252–259

Lide DR (1998) Handbook of chemistry and physics, 87 edn. CRC Press, Boca Raton. ISBN 0-8493-0594-2

Lund A, Olsson S, Bonora M, Lund E, Gustafsson H (2002) New materials for ESR dosimetry. Spectrochim Acta A 58:1301–1311

Moulton GC, Cernansky MP (1969) Electron spin resonance of X-irradiated single crystals of dl-tartaric acid at 77°K. J Chem Phys 51:2283–2284

Moulton GC, Cernansky B (1970) ESR studies of deuterated dl-tartaric acid × irradiated at 195°K. J Chem Phys 53:3022–3025

Murali S, Natarajan V, Venkataramani R, Sastry MD (2001) ESR dosimetry using inorganic materials: a case study of Li2CO3 and $CaSO_4$: Dy as prospective dosimeters. Appl Radiat Isot 55:253–258

Narasimha Rao DVG, Gordy W (1962) Electron spin resonance of an irradiated single crystal of deuterated DL-tartaric acid. J Chem Phys 36:1143–1145

Neuss JD, O'Brien MG, Frediani HA (1951) Sodium tartrate dihydrate as primary standard for Karl Fischer reagent. Anal Chem 23:1332–1333

Olsson SK, Lund E, Lund A (2000) Development of ammonium tartrate as an ESR dosimeter material for clinical purposes. Appl Radiat Isot 52:1235–1241

Polat M, Korkmaz M (2005) ESR identification of gamma-irradiated redoxon and determination of ESR parameters of radicals produced in irradiated ascorbic acid. Anal Chim Acta 535:331–337

Ramachandran GN, Radhakrishnan A (1951) Unit cell and space group of sodium tartrate $Na_2C_4H_4O_6$, $2H_2O$. Curr Sci 20:36

Regulla DF, Deffner U (1982) Dosimetry by ESR spectroscopy of alanine. Int J Appl Radiat Isot 33:1101–1114

Sharpe P (2003) Progress report on radiation dosimetry at NPL. Technical report, BIPM, CCRI(I)-03-14

Sharpe PHG, Rajendran K, Sephton JP (1996) Progress towards an alanine/ESR therapy level reference dosimetry service at NPL. Appl Radiat Isot 47:1171–1175

Tuner H, Korkmaz M (2009) Kinetic features of the radical species produced in gamma-irradiated dl-tartaric acid and the dosimetric potential of this acid. Radiat Res 172:120–128

Ustundag IO, Korkmaz M (2009) Spectroscopic, kinetic and dosimetric features of the radical species produced after radiodegradation of solid triclosan. Radiat Environ Biophys 48:159–167

Vestad TA, Malinen E, Lund A, Hole EO, Sagstuen E (2003) EPR dosimetric properties of formates. Appl Radiat Isot 59:181–188

Vickers PJ, Braybook J, Lawrence P, Gray K (2007) Detecting tartrate additives in foods: evaluating the use of capillary electrophoresis. J Food Compos Anal 20:252–256

William PB, Bhaskara PR (1976) Comparison of standards in the karl fischer method for water determination. Anal Chim Acta 84:149–155

Yordanov ND, Gancheva V (2004) Properties of the ammonium tartrate/EPR dosimeter. Radiat Phys Chem 69:249–256

Yordanov ND, Gancheva V, Georgieva E (2002) EPR and UV spectroscopic study of table sugar as a high-dose dosimeter. Radiat Phys Chem 65:269–276